Expedient and efficient: an Early Mesolithic composite implement from Krzyż Wielkopolski

Jacek Kabaciński[1,*], Auréade Henry[2], Eva David[3], Maxime Rageot[4,5,*], Carole Cheval[2], Małgorzata Winiarska-Kabacińska[6], Martine Regert[2], Arnaud Mazuy[2] & François Orange[7]

[1] Institute of Archaeology and Ethnology, Polish Academy of Sciences, Poznań, Poland

[2] Université Côte d'Azur, CNRS, CEPAM, Nice, France

[3] CNRS, UMR 7041 Laboratory ArScAn-AnTET, Nanterre, France

[4] Institut für vor- und frühgeschichtliche Archäologie und Provinzialrömische Archäologie, Ludwig-Maximilians-Universität München, Munich, Germany

[5] Department of Pre- and Protohistory, University of Tübingen, Germany

[6] Poznań Archaeological Museum, Poland

[7] Université Côte d'Azur, CCMA, Nice, France

[*] Authors for correspondence ✉ jacek.kabacinski@interia.pl & maxime.rageot@uni-tuebingen.de

OSM1: methods and detailed observations

X-ray analysis

X-ray analysis was conducted in neoMedica Medical Center in Poznań, Poland using standard digital medical equipment.

Radiocarbon dating

AMS ^{14}C radiometric analysis was performed in the Poznań Radiocarbon Laboratory in 2014 (Lab. No: Poz-60253). The dated material was an amorphous organic layer covering most of the artefact. It was removed with a scalpel from the bottom part of the point.

Technological analysis (É. David)

The analysis of the bone point combined low and high magnification microscopic observations of available parts of the artefact using a methodology developed in the CNRS 7041 Laboratory ArScAn-AnTET, France. The methodology was proposed at the end of the twentieth century (Vincent 1993) and develop recently as a proxy to examine the origin of technical change in the Stone Age (e.g. David & Kjällquist 2018). Technical diagnosis on

modified bone and shell uses several disciplinary fields in natural and human sciences to reconstruct past technologies. In this study, the identification of manufacturing/hafting techniques and the ergonomic use of the composite point is based on the artefact's biography as reconstructed from observing surfaces to see how worked planes overlap, organise and structure the material product (e.g. David & Valentin Eriksen 2021).

Results

According to the relatively high degree of transformation of the osseous part, it is rather difficult to identify whether it is made of bone or antler material. Visible longitudinal desiccation cracks reflect a substantial axially lamellar tissue, a characteristic of the osseous histological structure. The large alveolar pattern of the vascular (Volkmann) canals emerging from the external surface would possibly agree with bone material (Figure 5A; Laroche 2002). Moreover, the thickness of the hard bone which corresponds to that of the whole size of the visible tip, is greater than the thickness range usually observed for (red deer) antler if also measured from a long straight (beam) part. The X-ray image (Figure 3B) indicates that the basal end of the bone is made pointed, suggesting the use of a more or less regular splinter in the manufacture potentially using the shaft-wedge-splinter technique (David 2004).

Most probably, a long bone was thus split lengthwise to extract an elongated splinter, which was then regularised and/or sharpened into a point. Where the black thick layer is decayed, several striations remain visible on the bony surface and attest to that the bone shaft was worked lengthwise (Figure 5B). The X-ray profiles of the point (Figure 3B) also show that the splinter is quite irregular; probably that its edges were regularised once the splinter was obtained, as corroborated by some heavily marked rectilinear planes in the same delineation of the irregular lateral sides of the bone point itself, unless the bone was locally deeply sawn lengthwise in diverse areas before being split. Many of the evoked axial striations display variable depths suggesting the use of a coarse-grained stone (tool?) to work the bone. As they are parallel and somehow locally form quite a deep straight plane carving along over the area, they suggest that the bone was cut axially employing therefore either the grooving or the sawing techniques (David 2004) and/or that it was regularised in a wide lengthwise gesture using the grinding technique; all possibilities with the help of a stone grinder and/or a coarse-grained stone edge. The rough aspect of the bone surface might also have promoted then a better grip for adding black matter over the osseous surface.

In clear rupture with this regularised shape, the very tip of the bone point appears rather smooth, straight and symmetrical as if particularly shaped compared to the rest of the bone piece. Some slightly marked planes on the tip-end in surface suggest that the bone might have been initially shaped in facetted planes, each by working (grinding?) on the bone lengthwise before the item eventually became worn-out, ending with a crushed-smooth round-like tip-end.

Functional analysis (M. Winiarska-Kabacińska)

The active part of the point was analysed at the Traceology Laboratory of the Poznań Archaeological Museum, Poland. A standard methodology based on comparative studies of traces and residues observed on prehistoric artefacts and experimental tools was employed. This method of reconstruction of past activities performed by prehistoric groups was proposed already in the 1960s (Semenov 1964; Tringham *et al.* 1974; Keeley & Newcomer 1977) and developed later (e.g. Keeley 1980; Anderson-Gerfaud 1981; Moss 1983; Marreiros *et al.* 2015). In this study, two microscopes were used: a stereoscope microscope SZX9 and metallographic microscope Olympus BX53M with magnifications ranging from several tens to several hundred times.

Results

Functional analysis confirms that different parts of the point were elaborated with different techniques. Although partially covered by the black substance, microwear visible in the central part of the point's surface showed that it was scraped with the help of flint tool(s), most probably burins (Figure 6A–B), although the limited use of a coarse stone grinder may also have contributed to the patterns. Use-wear analysis also confirms that the tip of the point was worked in a completely different way. No traces of scraping were observed and it seems that part of the artefact was shaped and smoothed with the help of a fine-grained polisher (Figure 6E). There are some post-depositional traces visible on this part of the point in the form of a few elongated cuts (Figure 6C–D). The tip of the point (apex) is rounded with a damage in the shape of a triangular split, most probably as a result of percussion (Figure 6F). Rounding, associated with tip damage, were experimentally observed as a result of the repeated use of a bone point as a hunting weapon (Buc 2011; Bradfield 2015).

Xylological analysis (A. Henry)

Technological and anatomical analyses of the wood were restricted since the black amorphous layer was almost completely covering the shaft. We were however able to retrieve information from two areas where this layer was no longer preserved and the wood underneath was visible. This allowed the examination of the wood's transversal and longitudinal radial sections, respectively on the proximal end and the lateral side of the artefact. The analyses were performed with a stereomicroscope at a ×20 magnification and a reflected light microscope with natural and polarised light at ×100 and ×200 magnifications at the Traceology Laboratory of the Poznań Archaeological Museum, Poland. The taxonomic identification was made according to Schweingruber (1990).

The anatomical characteristics of the wood at magnifications ranging from ×20 to ×500 allowed a positive identification as *Pinus sylvestris* tp (Scots pine type): the wood is homoxylous, with resin canals and the early-late wood transition is abrupt. The cross-fields bear one large fenestriform pit (Table S1)**.** This wood type regroups the species *Pinus sylvestris*, *P. mugo* and *P. nigra*, which are impossible to discriminate based on their microscopic anatomy; however, we are most likely dealing with *P. sylvestris*, given the chrono- and biogeographical context, as well as the fact that the many cones identified at the site belong to *P. sylvestris* (Lityńska-Ząjąc 2014).

Table S1. Available elements for the taxonomical identification of the wood.

Section	Microscope used	Anatomical observations
Transversal	Stereomicroscope	Wood homoxylous; resin canals present; abrupt transition from early- to latewood
Longitudinal radial	Stereomicroscope; reflexion microscope	Cross-fields with pinoid pits, dentated walls in ray tracheids
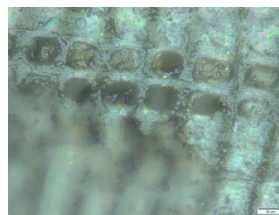
The wood shows excellent preservation, as indicators of wood degradation (hyphae, cell wall deformations caused by fungi etc.), which may have occurred during the taphonomical history of the object, were not observed. The anatomical regularity of the transversal and the radial sections, as well as the absence of radial grooves characteristic of reaction wood, suggest the use of straight-grained wood.

The growth rings show no curvature (almost flat), which indicates that the wooden rod used to make the object was extracted from a greater calibre, at some distance from the pith. The examination of the proximal end of the shaft shows that the wood section is of general quadrangular shape, suggesting few operatory steps, i.e. direct extraction of a rod of appropriate size following the direction of the fibres and its subsequent bevelling on the distal end in order to fit against the bone as shown by the X-ray analysis (Figure 3). However, the observation of the (incomplete) proximal end of the artefact did not allow assessing if the shaft becomes progressively wider or if what we observe actually corresponds to its maximal width/thickness.

In light of the information delivered by the xylological analysis, it is very likely that the primary exploitation of a suitable material (i.e. straight-grained and sound wood) represented more investment than its manufacture.

Fibre analysis and SEM micrographs (C. Cheval, A. Henry & F. Orange)

At a macroscopic level, the ligature is poorly preserved and visible only in a relict form over the area where the adhesive is no longer present. Microscopic examination of both longitudinal and cross-sectional samples is typically used to determine the nature of the fibres. A small sample was extracted under the stereomicroscope with a scalpel (Figure 4) and observed using a Tescan Vega 3 XMU scanning electron microscope (SEM) at the Centre of Applied Microscopy (CCMA, Nice).

Samples were observed either untreated, using the low vacuum mode of the SEM (pressure between 20 and 40Pa), or after carbon coating.
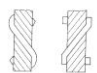
The distinction between plant and animal fibres (e.g. hairs) was possible thanks to Scanning Electron Microscope (SEM) observation, in longitudinal and transversal views (Janaway 1983). The natural twist of the fibres can provide complementary clues since it varies according to their nature; this direction is noted either Z or S in reference to the diagonal of the letter (Emery 1994), for example, flax and nettle natural twist is S whereas for hemp it is Z.

The dispersed, fragmentary nature of the observed fibre elements (a few filaments) did not allow to fully appreciate the degree of twisting. We were nevertheless able to observe several micro-samples at higher magnification ($\times 2000$) with the SEM (Figure 7–D), whose characteristics are summarised in Table S2.

These indicate that the fibres used in the manufacture of the point are of plant origin and more specifically, that they correspond to ligneous fibres, similar to those observed on a

sample of poplar bast from our reference collection (Figure 7E). The small, oval pits are characteristic of libriform fibres, which are present in poplar but also in a number of other angiosperms. The fibres' widths are also equivalent to those of poplar. It is however difficult to further characterize the bast from Krzyż, as only isolated fibres were available for the anatomical analysis. Within the experimental basts from our laboratory collection, wood rays and vessels are usually also observed, enabling a more precise taxonomic determination.

Table S2. Microscopic features of the fibre samples.

Micrographs	General appearance	Width (µm)	Flexural nodes (stalk fibre) (Y/N)	Overlapping scales (animal origin) (Y/N)	Twisting (white arrows in Figure 7)	Observations
Figure 7A	Ribbon-like, smooth	6–9	N	N	Z	Localized bulge (11µm) evoking a stalk fibre
Figure 7B	Ribbon-like	15–21	N	N	Z	
Figure 7C	Strap with curled edges	20–22	N	N	Not observed	Presence of oval pits. Some bulges
Figure 7D	Strap with curled edges	21 (average)	N	N	Z & S	Presence of oval pits

Molecular analyses (M. Rageot, A. Mazuy & M. Regert)

In order to determine the nature of the hafting adhesive, gas chromatography–mass spectrometry (GC-MS) was applied to a micro sample of the black organic layer covering the object. This methodology is commonly employed for the characterisation of organic amorphous residues and well-adapted to the identification of organic lipidic or resinous materials such as the one covering the artefact.

The sample was extracted with dichloromethane (1mg.mL^{-1}, HPCL grade) and dried under a gentle nitrogen beam at 40°C. The extract was then derivatised in a mixture of 50µl of BSTFA +1%TMCS, 4µL of pyridine and 1µL of dichloromethane for 30 minutes at 70°C. After evaporation until dryness under a gentle stream of nitrogen at 40°C, the sample was diluted in dichloromethane (1 mg.mL^{-1}, HPCL grade) before GC-MS analysis (injection of

1μl). GC-MS analyses were performed using a Shimadzu GC2010plus QP2010ultra. The GC was equipped with a splitless injector and fitted with an Agilent J&W DB-5MS column (30m × 0.25mm i.d.; 0.25μm film thickness). Helium was used as carrier gas with a constant head flow rate of 3mL min^{-1} at 300°C. The oven temperature was ramped from 50°C (held isothermally for 2 minutes) to 150°C at 10°C min^{-1}, and then increased to 320°C at 4°C min^{-1} (held isothermally for 15 minutes).

Mass spectra were acquired using electron ionisation at 70 eV. The mass range was scanned on the range *m/z* 50–950 in 0.6 s. The temperature of the ion source was fixed at 200°C and that of the transfer line at 250°C. Mass spectra were matched against those of authentic standards (betulin, betulinic acid, lupeol, lupenone, oleanolic acid and β-amyrin), by using the NIST library and data from previous works (Binder *et al.* 1990; Hayek *et al.* 1990; Aveling & Heron 1998; Li *et al.* 1998; Regert *et al.* 1998; Garnier 1999; Lavoie 2001; Rageot 2015).

Results

GC-MS of the adhesive substance revealed the presence of two main groups of chemical constituents: triterpenoids that are by far the most abundant components eluting after 40 min (compounds 1 to 21) and simple and complex (diacids, unsaturated fatty acids) fatty acids with retention times lower than 42 minutes.

The 20 triterpenoid components identified have all a pentacyclic skeleton of lupane or oleanane type (Figure 8 and Table S3).

Their association is characteristic of birch bark tar (Binder *et al.* 1990; Hayek *et al.* 1990; Charters *et al.* 1993; Aveling & Heron 1998; Regert *et al.* 1998; 2019; Rageot 2015; Rageot *et al.* 2019; 2021): oleanolic-3-acetate (5), betulinic acid (7), oleanolic acid (8), betulin (9), betulinic aldehyde (10), erythrodiol (13), lupeol (14) and b-amyrin (16) have all been identified in different birch barks (BioMarkers - BM, réf) while allobetulin (6), oleandien-28-oic acid (18), lupa-2,20 (29)-dien-28-ol (19), α-betulin I (20) and lupa-2,20 (29)-dien (21) are known to be formed by transformation and alteration of birch bark (degradation markers (DM)) following a series of various mechanisms including oxidation, dehydration, cycloisomerisation (Rageot *et al.* 2019). Most of them are formed during the process of transformation of birch bark in tar during heating but some of them may also provide evidence of post-depositional alteration. Lupenone (15) is naturally present in birch bark, but its concentration may increase during heating by oxidation of lupeol (14). Two other constituents present at low amount, betulin-28-caffeate (1) and erythrodiol-28-caffeate (2)

could result from a reaction between triterpene biomarkers and phenolic monomers from suberin during tar manufacturing. The triterpene caffeates are usually known as biomarkers in birch bark, especially oleanolic acid and betulin derivatives. However, the caffeates are described for the 3β position of the triterpenes (Pan *et al.* 1994; Krasutsky 2006).

The number and amount of triterpenoid biomarkers that make up more than 85 % of the triterpenoid extract (compounds 5, 7, 8, 9, 10, 13, 14 and 16) provide evidence of the limited impact of natural and/or heat degradations.

Several even and odd numbers of fatty acids (C_{16}–C_{22}) and diacids (C_{18}–C_{22}) were also identified in low amounts in the archaeological sample. Their presence may result from the degradation of suberin during the manufacturing process (Ekman 1983; Rageot 2015). The preservation of such fatty acids together with the high percentage of triterpenoid biomarkers suggest that the tar was produced in soft heating conditions as experienced in laboratory conditions by heating birch bark of *Betula pendula* for 10 minutes from room temperature to 350°C (Rageot 2015; Rageot *et al.* 2019). It is therefore likely that the tar covering the wooden shaft from Krzyż corresponds to a material produced by a soft heating process, chemically close to the 'first bark exudate'.

Table S3. List of triterpenoid components identified. The percentages are relative to the % in the triterpenoid fraction. DM = degradation marker; BM = BioMarker; PT = pentacyclic triterpenoids.

					Laboratory First tar exudations	Birch bark tar from Krzyz
Chemical families		% Fatty acids (C16 to C22)			13	2
		% Diacids (C18 TO C22)			6	8
		% Pentacyclic triterpenes (lupanes and oleananes)			76	78
		% Others			5	12
Pentacyclic triterpenes		Biomarkers (% BM/PT)			58	85
		Degadation markers (% DM/PT)			42	15
	Number	**Name**	**Skeleton**	**Type of marker**	**% /PT**	**% /PT**
	21	Lupa-2,20(29)-dien	lupane	DM	2.36	0.42
		Lupa-2,20(29)-dien* (isomer)	lupane	DM	1.03	tr
	20	α-betulin I	α-lupane	DM	4.27	0.60
		b386	lupane	DM	_	0.29
		Allobetul-2-en	oleanane	DM	_	tr
	19	Lupa-2,20(29)-dien-28-ol	lupane	DM	7.32	4.49
		Lupa-2,20(29)-dien-28-ol* (isomer)	lupane	DM	1.89	1.20
	18	Olean-dien-28-oic acid	oleanane	DM	1.24	tr
	17	Lupa-2,20(29)-dien-28-oic acid	lupane	DM	3.29	0.87
	16	β-Amyrin	oleanane	BM	4.38	0.77
	15	Lupenone	lupane	DM	_	1.14
		b418 (oleanol)	oleanane	DM	1.94	tr
	14	Lupeol TMS	lupane	BM	14.18	9.55
	13	Erythrodiol TMS	oleanane	BM	1.54	1.42
	12	b447 (erythrodiol deriv?)	oleanane	DM	9.91	5.20
	11	Betulone	lupane	DM	3.31	tr
	10	Betulinic aldehyde	lupane	BM	_	0.96
	9	Betulin	lupane	BM	29.68	68.41
	8	Oleanolic acid	oleanane	BM	1.94	_
	7	Betulinic acid	lupane	BM	4.45	2.52
	6	Allobetulin	oleanane	DM	3.93	tr
	5	Oleanolic acid 3-acetate	oleanane	BM	1.65	0.99
	4	Betulinic acid methyl ester	lupane	DM	1.11	_
	3	Betulin 28-acetate	lupane	DM	0.58	0.37
	2	Erythrodiol 28-caffeate	oleanane	DM	tr	0.32
	1	Betulin 28-caffeate	lupane	DM	tr	0.47

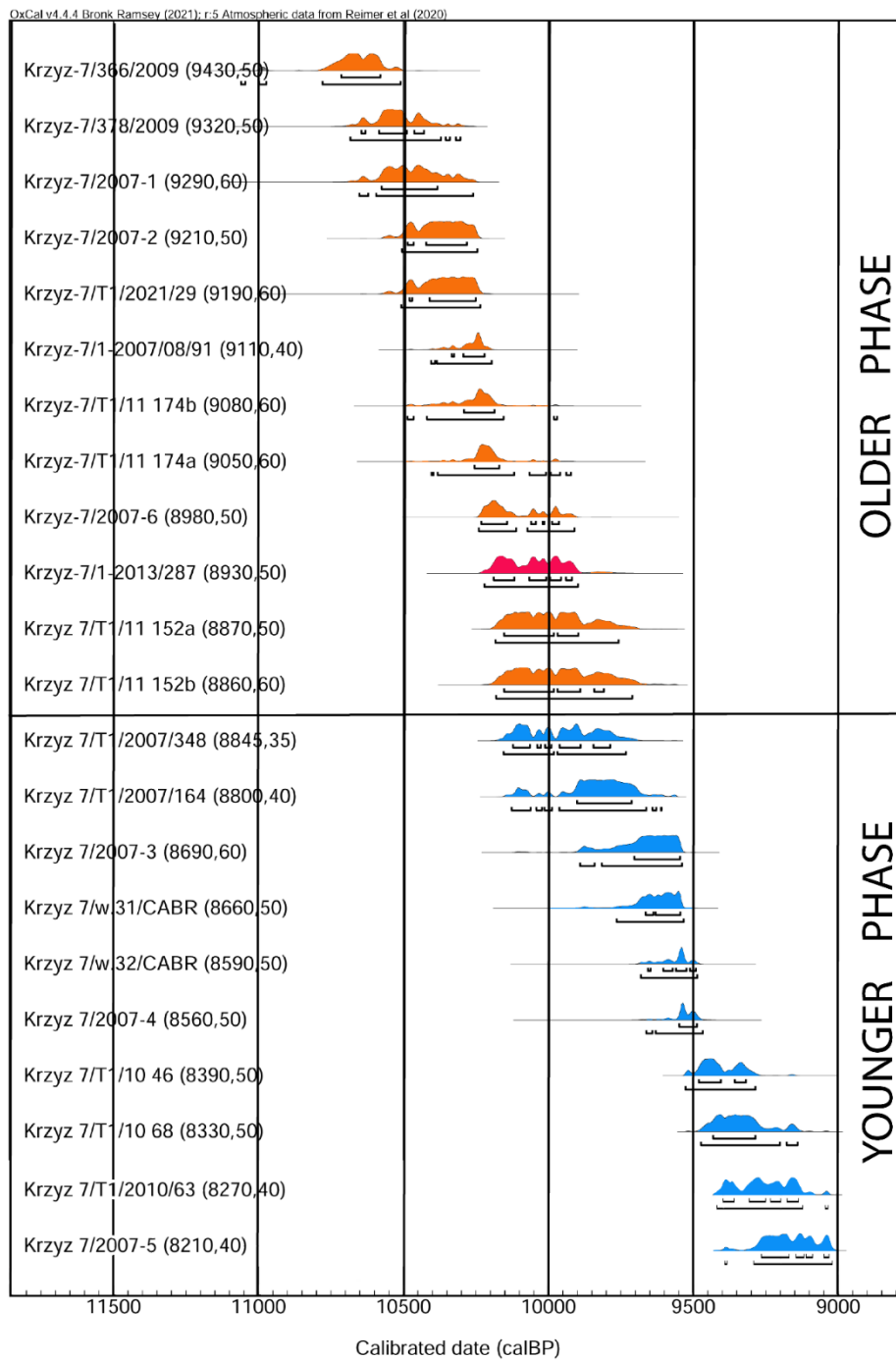**OSM2: radiocarbon dates for Krzyż Wielkopolski, Site 7**

Figure S1. Calibration of radiocarbon dates for Krzyż Wielkopolski, site 7 (calibrated in OxCal (v4.4.4) using the IntCal20 calibration curve (Bronk Ramsey 2009; Reimer et al. 2020).

Table S4. Description of radiocarbon dated samples from Krzyż Wielkopolski, site 7. Calibrated in OxCal (v4.4.4) using the IntCal20 calibration curve (Bronk Ramsey 2009; Reimer *et al.* 2020)

Phase	No.	Sample number	Laboratory number	Material dated	^{14}C age bp	Cal BP				Median	Remarks
						probablity 68.2%		probability 95.4%			
						from	to	from	to		
Older phase	1	Krzyz-7/366/2009	Poz-34354	bone (carbonate)	9430±50	10714	10580	11060	10510	10660	trench 1/2007, season 2009, metacarpal bone of horse
	2	Krzyz-7/378/2009	Poz-34352	antler (collagen)	9320±50	10645	10429	10683	10303	10523	trench 1/2007, season 2009, elk antler
	3	Krzyż-7/2007-1	Poz-27405	charcoal	9290±60	10575	10382	10652	10259	10468	trench 1/2007, N profile
	4	Krzyż-7/2007-2	Poz-27406	charcoal	9210±50	10485	10282	10505	10245	10370	trench 1/2007, N profile
	5	Krzyż-7/T1/2012/29	Poz-52318	charcoal	9190±60	10479	10250	10507	10235	10357	trench 1/2012, below mandible of elk
	6	Krzyż 7/1 2007/08/91	Poz-60335	horn (collagen)	9110±40	10334	10220	10405	10196	10256	trench 1/2007, season 2008, auroch horn
	7	Krzyż-7 T1/11 174b	Poz-46204	bone (collagen)	9080±60	10291	10186	10486	9970	10239	trench 1/2011, adze made of elk tibia bone
	8	Krzyż 7 T1/11 174a	Poz-46207	wood (*Populus*)	9050±60	10255	10169	10403	9922	10216	trench 1/2011, handle of elk' tibia adze (see above)
	9	Krzyż-7/2007-6	Poz-27419	antler (collagen)	8980±50	10231	9964	10240	9911	10152	trench 1/2007, season 2008, zoomorphic 'magic stick', red deer antler
	10	Krzyż 7/1-2013/287	Poz-60253	birch tar	8930±50	10188	9919	10220	9898	10048	trench 1/2013, composite point
	11	Krzyż 7 T1/11 152a	Poz-46206	wood (*Cornus*)	8870±50	10153	9897	10183	9758	9997	trench 1/2011, handle of red deer antler adze (see below)
	12	Krzyż 7 T1/11 152b	Poz-46205	antler (collagen)	8860±60	10153	9809	10180	9711	9967	trench 1/2011, adze made of red deer antler
Younger phase	13	Krzyż-7/T1/2007/348	Poz-52319	wood (*Cornus*)	8845±35	10122	9789	10154	9732	9947	trench 1/2007, season 2008, handle of red deer antler adze
	14	Krzyż-7/T1/2007/164	Poz-52321	bone (collagen)	8800±40	9901	9713	10127	9609	9827	trench 1/2007, season 2009, femur bone of dog
	15	Krzyż-7/2007-3	Poz-27487	charcoal	8690±60	9704	9545	9891	9539	9653	trench 1/2007, N profile
	16	Krzyż 7 w. 31/CARB	Poz-12959	bone (carbonate)	8660±50	9665	9544	9764	9534	9619	adze made of aurochs metapodial bone
	17	Krzyż 7 w. 32/CARB	Poz-12919	bone (carbonate)	8590±50	9656	9491	9681	9486	9549	adze made of aurochs metapodial bone
	18	Krzyż-7/2007-4	Poz-27416	charcoal	8560±50	9549	9488	9662	9467	9530	trench 1/2007, N profile

	19	Krzyż 7 T1/10 46	Poz-46209	fruit of *Corylus avellana*	8390±50	9481	9319	9527	9286	9420	trench 1/2010
	20	Krzyż 7 T1/10 68	Poz-46208	fruit of *Corylus avellana*	8330±50	9432	9286	9473	9140	9348	trench 1/2010
	21	Krzyż-7/T1/2010/63	Poz-52309	fruit of *Corylus avellana*	8270±40	9402	9139	9423	9037	9260	trench 1/2010
	22	Krzyż-7/2007-5	Poz-27418	charcoal	8210±40	9268	9033	9395	9021	9174	trench 1/2007, N profile

References

ANDERSON-GERFAUD, P. 1981. Contribution méthodologique Ã l'analyse des microtraces d'utilisation sur les outils préhistoriques. Unpublished PhD dissertation, Université de Bordeaux.

AVELING, E.M. & C. HERON. 1999. Chewing tar in the Early Holocene: an archaeological and ethnographic evaluation. *Antiquity* 73: 579–84. https://doi.org/10.1017/S0003598X00065133

BINDER, D., G. BOURGEOIS, F. BENOIST & C. VITRY. 1990. Identification de brai de bouleau (*Betula*) dans le néolithique de Giribaldi (Nice, France) par la spectrométrie de masse. *Revue d'Archéométrie* 14: 37–42. https://doi.org/10.3406/arsci.1990.881

BRADFIELD, J. 2015. Use-trace analysis of bone tools: a brief overview of four methodological approaches. *South African Archaeological Bulletin* 70: 3–14.

BRONK RAMSEY, C. 2009. Bayesian analysis of radiocarbon dates. *Radiocarbon* 51: 337–60. https://doi.org/10.1017/S0033822200033865

BUC, N. 2011. Experimental series and use-wear in bone tools. *Journal of Archaeological Science* 38: 546–57. https://doi.org/10.1016/j.jas.2010.10.009

CHARTERS, S. *et al*. 1993. Identification of an adhesive used to repair a Roman jar. *Archaeometry* 35: 91–101. https://doi.org/10.1111/j.1475-4754.1993.tb01025.x

DAVID, É. 2004. Transformation des matières dures d'origine animale dans le Mésolithique de l'Europe du Nord, in D. Ramseyer (ed.) *Industrie de l'os préhistorique: matières et techniques* (Fiches de la Commission de Nomenclature de l'Industrie Osseuse XI): 113–49. Paris: Éditions de la Société Préhistorique Française.

DAVID, É. & M. KJÄLLQUIST. 2018. Transmission of knowledge, crafting and cultural traditions, interregional contact and interaction, 7300 cal BC: a study of worked material from Norje Sunnansund, Sweden, in K. Knutsson, H. Knutsson, J. Apel & H. Glørstad (ed.) *Technology of early settlement of Northern Europe: transmission of knowledge and culture*: 231–76. Sheffield: Equinox.

DAVID, É. & B. VALENTIN ERIKSEN. 2021. Antler tool's biography shortens time frame of Lyngby-axes to the last stage of the Late-Glacial, in S. Gaudzinski-Windheuser & O. Jöris (ed.) *The beef behind all possible pasts: the tandem festschrift in honour Elaine Turner and Martin Street* (Monographien des Römisch-Germanischen Zentralmuseums, Band 157): 639–56. Mainz: Schnell & Steiner.

EKMAN, R. 1983. The Suberin monomers and triterpenoids from the outer bark of *Betula verrucosa Ehrh. Holzforschung* 37: 205–211. https://doi.org/10.1515/hfsg.1983.37.4.205

EMERY, I. 1994. *The primary structures of fabrics: an illustrated classification*. New York: Thames & Hudson.

GARNIER, N. 1999. Détermination de la structure moléculaire d'écorces actuelles et d'adhésifs archéologiques par chromatographie en phase gazeuse couplée à la spectrométrie de masse (CPG-SM), Spectrométrie, Analyse et Physicochimie Organique. Unpublished Master's dissertation, Université Paris VI.

HAYEK, E.W.H. *et al*. 1990. Identification of archaeological and recent wood tar pitches using gas chromatography/mass spectrometry and pattern recognition. *Analytical Chemistry* 62: 2038–43. https://doi.org/10.1021/ac00217a026

JANAWAY, R. 1983. Textile fibre characteristics preserved bymetal corrosion: the potential of S.E.M. studies. *The Conservator* 7: 48–52. https://doi.org/10.1080/01410096.1983.9994979

KEELEY, L. 1980. *Experimental determination of stone tool uses: a microwear analysis*. Chicago (IL): University of Chicago Press.

KEELEY, L. & M. NEWCOMER. 1977. Micro-wear analysis of experimental flint tools: a test case. *Journal of Archaeological Science* 4: 29–62. https://doi.org/10.1016/0305-4403(77)90111-X

KRASUTSKY, P.A. 2006. Birch bark research and development. *Natural Product Reports* 23: 919–42. https://doi.org/10.1039/B606816B

LAROCHE, M. 2002. Circulation intraosseuse: de la physiologie à la pathologie. *Revue du Rhumatisme* 69: 484–91. https://doi.org/10.1016/S1169-8330(02)00325-3

LAVOIE, S. 2001. Contribution à la synthèse de dérivés de l'acide bétulinique à partir du betulinol extrait de l'ecorce du bouleau blanc (*Betula papyrifera*). Unpublished Master's dissertation, Université du Québec à Chicoutimi.

LI, T.-S., J.-X. WANG & X.-J. ZHENG. 1998. Simple synthesis of allobetulin, 28-oxyallobetulin and related biomarkers from betulin and betulinic acid catalysed by solid acids. *Journal of the Chemical Society*, *Perkin Transactions 1*: 3957–66. https://doi.org/10.1039/A806735J

LITYŃSKA-ZAJĄC, M. 2014. Badania archeobotaniczne w Krzyżu Wielkopolskim, in J. Kabaciński (ed.) Społeczności łowiecko-zbierackie wczesnego mezolitu środkowej części Pradoliny Toruńsko-Eberswaldzkiej: 238–78. Unpublished manuscript, Instytut Archeologii i Etnologii PAN, Poznań.

MARREIROS, J.M., J.F. GIBAJA & N. FERREIRA BICHO. 2015. *Use-wear and residue analysis in archaeology*. New York: Springer. https://doi.org/10.1007/978-3-319-08257-8

Moss, E.H. 1983. *The functional analysis of flint implements. Pincevent and Pont d'Ambon: two cases from the French Final Palaeolithic* (British Archaeological Reports International Series 177). Oxford: British Archaeological Reports. https://doi.org/10.30861/9780860542278

Pan, H., L.N. Lundgren & R. Andersson. 1994. Triterpene caffeates from the bark of Betula pubescens. *Phytochemistry* 37: 795–99. https://doi.org/10.1016/S0031-9422(00)90360-1

Rageot, M. 2015. Les substances naturelles en Méditerranée Nord-occidentale (VIe-Ier millénaire BCE): chimie et archéologie des matériaux exploités pour leurs propriétés adhésives et hydrophobes. Unpublished PhD dissertation, Université Nice-Sophia Antipolis.

Rageot, M. *et al*. 2019. Birch bark tar production: experimental and biomolecular approaches of a common and widely used prehistoric adhesive. *Journal of Archaeological Method and Theory* 26: 276–312. https://doi.org/10.1007/s10816-018-9372-4.

– 2021. Management systems of adhesive materials throughout the Neolithic in the north-west Mediterranean. *Journal of Archaeological Science* 126: 105309. https://doi.org/10.1016/j.jas.2020.105309

Regert, M. *et al*. 1998. Identification of Neolithic hafting adhesives from two lake dwellings at Chalain (Jura, France). *Ancient Biomolecules* 2: 81–97.

– 2019. Birch bark tar in the Roman world: the persistence of an ancient craft tradition? *Antiquity* 93: 1553–68. https://doi.org/10.15184/aqy.2019.167

Reimer, P. *et al.* 2020. The IntCal20 Northern Hemisphere radiocarbon age calibration curve (0–55 cal kBP). *Radiocarbon* 62: 725–57. https://doi.org/10.1017/RDC.2020.41

Schweingruber, F.-H. 1990. *Microscopic wood anatomy*. Bern: Paul Haupt.

Semenov, S.A. 1964. *Prehistoric technology: an experimental study of the oldest tools and artefacts from traces of manufacture and wear*. London: Cory, Adams & Mackay.

Tringham, R. *et al*. 1974. Experimentation in the formation of edge damage: a new approach to lithic analysis. *Journal of Field Archaeology* 1: 171–96. https://doi.org/10.1179/jfa.1974.1.1-2.171

Vincent, A. 1993. *L'outillage osseux au Paléolithique moyen: une nouvelle approche*. Unpublished PhD dissertation, Université-Nanterre Paris X.